# DEVELOPMENT OF DNA APTAMERS AGAINST BipD ANTIGEN OF Burkholderia pseudomallei FOR DIAGNOSTIC APPLICATIONS

# **KASTURI A/P SELVAM**

# UNIVERSITI SAINS MALAYSIA

2025

# DEVELOPMENT OF DNA APTAMERS AGAINST BipD ANTIGEN OF Burkholderia pseudomallei FOR DIAGNOSTIC APPLICATIONS

by

### **KASTURI A/P SELVAM**

Thesis submitted in fulfilment of the requirements for the degree of Doctor of Philosophy

September 2025

#### **ACKNOWLEDGEMENT**

I am profoundly grateful to the Almighty for granting me the opportunity to pursue a Doctor of Philosophy and for providing me with the strength to complete this journey. First and foremost, I extend my heartfelt gratitude to my supervisor, Associate Professor Dr. Aziah binti Ismail, for her invaluable guidance and constant encouragement throughout my academic endeavours. I want to express my sincere appreciation to my co-supervisors, Professor Dr. Habibah binti A. Wahab, Associate Professor Dr. Azian binti Harun, and Dr. Khairul Mohd Fadzli bin Mustaffa, as well as to research officers, Dr. Muhammad Hafiznur bin Yunus and Mr. Muhammad Fazli bin Khalid, for their constructive feedback and insightful comments, which have significantly enriched the quality of my study.

My deepest gratitude goes to my parents, Selvam A/L A Sinnappan and Letchumi A/P Appavoo Asari Perumal, for their unwavering support and encouragement. Their sacrifices and faith in my journey have been my greatest sources of strength and motivation. I want to express my sincere appreciation to my friends for their technical assistance, constant encouragement, and emotional support. I am also grateful to the laboratory staff of the Institute for Research in Molecular Medicine (INFORMM), Universiti Sains Malaysia (USM), for their invaluable contributions. Lastly, I extend my appreciation to the Graduate Student Financial Assistance (GRA-ASSIST) for providing me with financial support for one year, as well as to the Higher Institution Centre of Excellence (HICoE), Ministry of Higher Education, Malaysia, for supporting my study.

#### **TABLE OF CONTENTS**

ACK	NOWLE	DGEMENT	ii
TAB	LE OF C	ONTENTS	iii
LIST	OF TAB	LES	X
LIST	OF FIG	URES	xi
LIST	OF SYM	IBOLS	XV
LIST	OF ABB	REVIATIONS	xvi
LIST	OF APP	ENDICES	xxi
ABS	TRAK		xxii
ABS	TRACT		xxiv
СНА	PTER 1	INTRODUCTION	1
1.1	Study ba	ackground	1
1.2	Problem	statement	2
1.3	Rational	le of study	3
1.4	Scope of	f study	4
1.5	Study ol	ojectives	7
	1.5.1	General objective	7
	1.5.2	Specific objectives	7
СНА	PTER 2	LITERATURE REVIEW	8
2.1	Melioid	osis: an overview	8
	2.1.1	Global epidemiology of melioidosis	8
	2.1.2	Status of melioidosis in Malaysia	12
2.2	Etiologi	cal agent of melioidosis	14
	2.2.1	Taxonomy of B. pseudomallei	15
	2.2.2	Classification of Burkholderia species	17
2.3	Transmi	ssion mode of <i>B. pseudomallei</i>	17

2.4	Risk fac	tors of melioidosis	. 20
2.5	Pathoge	nesis of melioidosis	. 21
	2.5.1	Attachment and invasion of <i>B. pseudomallei</i>	. 21
	2.5.2	Phagosomal escape and replication of <i>B. pseudomallei</i>	. 23
	2.5.3	Dissemination and multinucleated giant cell (MNGC) formation	. 23
2.6	Clinical	manifestation of melioidosis	. 24
	2.6.1	Acute infection	. 24
	2.6.2	Chronic infection	. 26
	2.6.3	Latent infection	. 26
2.7	Treatme	nt of melioidosis	. 26
2.8	Preventi	on of melioidosis	. 29
2.9	Laborato	ory diagnosis of melioidosis	. 30
	2.9.1	Culture	. 30
	2.9.2	Antibody detection	. 34
	2.9.3	Nucleic acid detection	. 35
	2.9.4	Antigen detection	. 35
2.10	T3SS of	B. pseudomallei	. 38
	2.10.1	BipD protein: a promising biomarker for melioidosis diagnostics	. 40
2.11	Aptamer	: a new frontier in diagnostics	. 41
	2.11.1	Comparison between aptamers over antibodies	. 44
	2.11.2	SELEX	. 47
	2.11.3	Application of aptamers in bacterial diagnostics	. 50
	2.11.4	Molecular docking and MD simulations	. 54
	2.11.5	Commercially available aptamer products	. 56
2.12	ELONA		. 57
2.13	Electroc	hemical aptasensor	. 60

	2.13.1	Immobilisation chemistry of aptamer onto the electrode surface	62
	2.13.2	Electrochemical transduction techniques	65
		2.13.2(a) Voltammetry	65
		2.13.2(b) EIS	66
	2.13.3	Application of electrochemical aptasensors in bacterial diagnostics	68
2.14	Summar	y of literature review	70
		EXPRESSION AND PURIFICATION OF RECOMBINAN N	
3.1	Introduc	tion	71
3.2	Methods	S	72
	3.2.1	Construction of recombinant plasmid	73
	3.2.2	Preparation of competent cells	75
	3.2.3	Transformation of the recombinant plasmid into competent cells	75
	3.2.4	Expression of recombinant BipD protein	76
	3.2.5	SDS-PAGE	77
	3.2.6	Purification of recombinant BipD protein	78
		3.2.6(a) Buffer exchange	78
	3.2.7	Purity analysis of recombinant BipD protein	79
3.3	Results.		80
	3.3.1	Expression of recombinant BipD protein	80
	3.3.2	Purification of recombinant BipD protein	83
3.4	Discussi	on	86
_	PTER 4 OMBINA	ISOLATION OF DNA APTAMERS TARGETING NT BipD PROTEIN	89
4.1	Introduc	tion	89
4.2	Methods	S	90

	4.2.1	Synthesis of DNA library and primers90
	4.2.2	Coupling of recombinant BipD protein to the NHS-activated agarose beads
	4.2.3	In-vitro selection of DNA aptamers targeting recombinant BipD protein
	4.2.4	Regeneration of DNA library
		4.2.4(a) Optimisation of PCR cycles
		4.2.4(b) Large-scale PCR99
		4.2.4(c) Large-scale asymmetric PCR99
		4.2.4(d) Lambda exonuclease digestion
		4.2.4(e) Ethanol precipitation
	4.2.5	SELEX monitoring
	4.2.6	Cloning, Sanger sequencing and phylogenetic analysis
		4.2.6(a) Preparation of competent cells
		4.2.6(b) Ligation of amplified DNA into the cloning vector 104
		4.2.6(c) Introduction of the ligated vector into competent cells
		4.2.6(d) Blue-white screening
		4.2.6(e) Sanger sequencing and phylogenetic analysis108
	4.2.7	Statistical analysis
4.3	Results	
	4.3.1	Assessment of recombinant BipD protein coupling onto NHS-activated agarose beads
	4.3.2	Regeneration of DNA library
	4.3.3	SELEX monitoring
	4.3.4	Cloning and phylogenetic analysis
4.4	Discussion	on118

		EVALUATION OF BINDING AFFINITY AND SPECI AMERS	
5.1	Introduc	ction	123
5.2	Methods	S	124
	5.2.1	Binding affinity of DNA aptamers	126
	5.2.2	Bacterial culture	127
	5.2.3	Preparation of bacterial lysates	128
	5.2.4	Specificity of DNA aptamers	129
	5.2.5	Statistical analysis	129
5.3	Results.		130
	5.3.1	Assessment of binding affinity of DNA aptamers	130
	5.3.2	Biochemical identification of bacteria	132
	5.3.3	Evaluation of the specificity of DNA aptamers	134
5.4	Discussi	ion	137
_	APTER 6 AMERS A	PREDICTION OF INTERACTION BETWEEN DNA AND BipD PROTEIN	139
6.1	Introduc	etion	139
6.2	Methods	S	140
	6.2.1	Obtaining the tertiary structure of BipD protein	140
	6.2.2	Modelling the tertiary structure of DNA aptamers	141
	6.2.3	Molecular docking through AutoDock Vina	143
	6.2.4	MD simulations	143
6.3	Results.		144
	6.3.1	Predicted tertiary structure of the BipD protein	144
	6.3.2	Predicted tertiary structure of DNA aptamers	150
	6.3.3	Molecular docking	152
	6.3.4	MD simulations	154
6.4	Discussi	ion	165

	ASENSO	R FOR MELIOIDOSIS DIAGNOSTICS	171
7.1	Introduc	etion	171
7.2	Methods	S	172
	7.2.1	Electrochemical cleaning of SPGEs	174
	7.2.2	Construction of electrochemical aptasensor	174
	7.2.3	Electrochemical measurement	175
	7.2.4	Optimisation of aptamer concentration for electrochemical aptasensor	176
	7.2.5	Reproducibility of the electrochemical aptasensor	176
	7.2.6	Sensitivity of the electrochemical aptasensor	176
	7.2.7	Specificity of the electrochemical aptasensor	177
	7.2.8	Detection of BipD protein in spiked serum	177
	7.2.9	Statistical analysis	177
7.3	Results.		178
	7.3.1	Activation of bare SPGEs	178
	7.3.2	Optimisation of the aptamer concentration	180
	7.3.3	Characterisation of the electrochemical aptasensor	182
	7.3.4	Reproducibility of the electrochemical aptasensor	184
	7.3.5	Specificity of the electrochemical aptasensor	186
	7.3.6	Determination of the LoD of the electrochemical aptasensor	188
7.4	Discussi	ion	190
СНА	PTER 8	GENERAL DISCUSSION	195
СНА	PTER 9	CONCLUSION AND FUTURE RECOMMENDATIONS	199
9.1	Conclus	ion	199
9.2	Future r	ecommendations	200
REF	ERENCE	S	201
APPI	ENDICES		

# LIST OF PUBLICATIONS SCIENTIFIC PRESENTATIONS AWARDS

#### LIST OF TABLES

	Pag
Table 2.1	Taxonomy of <i>B. pseudomallei</i> 1
Table 2.2	Melioidosis treatment guideline
Table 2.3	Summary of representative diagnostic methods for melioidosis3
Table 2.4	Comparison between aptamers and antibodies
Table 2.5	Application of aptamers in bacterial detection5
Table 2.6	Application of electrochemical aptasensors in bacterial detection6
Table 4.1	Conditions employed in SELEX to enhance the stringency of DNA aptamer selection
Table 4.2	Master mixture for optimisation of the number of PCR cycles9
Table 4.3	Master mixture for large-scale PCR
Table 4.4	Master mixture for large-scale asymmetric PCR10
Table 4.5	Master mixture for PCR screening of white colonies10
Table 4.6	List of DNA aptamers targeting recombinant BipD protein and their frequencies
Table 5.1	Summary of biochemical test results for <i>B. pseudomallei</i> , <i>S.</i> Typhi, <i>S. flexneri</i> , <i>E. coli</i> , and <i>K. pneumoniae</i>
Table 6.1	Structural validation of the crystal structures of the BipD protein14
Table 6.2	Hydrogen bond occupancy analysis for all three complexes16
Table 6.3	List of nucleotides of the aptamer and amino acids of the protein that are involved in the hydrogen bonds for all three complexes

#### **LIST OF FIGURES**

	Pag
Figure 1.1	Flow chart of the study
Figure 2.1	Global distribution and reporting of melioidosis1
Figure 2.2	Top 25 countries with the highest predicted incidence of melioidosis due to environmental suitability for <i>B. pseudomallei</i> and the increase in the prevalence of diabetes mellitus.
Figure 2.3	States in Malaysia with a high incidence of melioidosis are highlighted in red boxes.
Figure 2.4	Transmission routes of <i>B. pseudomallei</i> .
Figure 2.5	Intracellular lifestyle of <i>B. pseudomallei</i>
Figure 2.6	Clinical manifestations of melioidosis
Figure 2.7	Colony characteristics of <i>B. pseudomallei</i> on <b>(A)</b> sheep blood agar; <b>(B)</b> MacConkey agar; and <b>(C)</b> Ashdown's agar
Figure 2.8	InBios AMD kit
Figure 2.9	The predicted structure of the Type III Secretion System 3 (T3SS-3) of <i>Burkholderia pseudomallei</i> consists of two main component39
Figure 2.10	Aptamer conformational recognition of its targets to form an aptamer-target complex
Figure 2.11	A general scheme of the SELEX protocol comprises four main steps:  (i) binding of library sequences to the target; (ii) washing to remove unbound sequences; (iii) elution of bound sequences; and (iv) amplification of eluted sequences that served as a new library for the next SELEX cycle.
Figure 2.12	Aptamer development and its application in bacteriology from 1990 to 2023
Figure 2.13	Direct and sandwich ELONA approaches

Figure 2.14	Three key components of an aptasensor
Figure 2.15	Common techniques for aptamer immobilisation on sensing interfaces
Figure 2.16	Three-electrode electrochemical measurement setup, comprising a working electrode, reference electrode, and counter electrode67
Figure 3.1	Outline of the expression and purification of the recombinant BipD protein
Figure 3.2	Construction of recombinant plasmid (pRSET A-BipD) using SnapGene software (version 7.1.1)
Figure 3.3	SDS-PAGE analysis of <b>(A)</b> supernatant and <b>(B)</b> pellet of cell lysates
Figure 3.4	SDS-PAGE profiles for <b>(A)</b> flow through, washed, and <b>(B-C)</b> eluted fractions after protein purification using Ni-NTA agarose resin84
Figure 3.5	Evaluation of purified recombinant BipD protein through (A) SDS-PAGE, and (B) western blotting
Figure 4.1	Coupling of recombinant BipD protein to Pierce <sup>TM</sup> NHS-activated agarose beads
Figure 4.2	Agarose bead-based SELEX involves four main steps95
Figure 4.3	Coupling efficiency of recombinant BipD protein onto NHS-activated agarose beads was evaluated through enzyme-linked immunoassay (ELISA)
Figure 4.4	(A) 4% agarose gel profile for the number of PCR cycles optimisation using elution from the first-based SELEX cycle
Figure 4.5	The enrichment of DNA targeting the recombinant BipD protein was evaluated through ELONA
Figure 4.6	(A) 1% (w/v) agarose gel profile of PCR products of 19 representative white colonies
Figure 5.1	ELONA protocol for <b>(A)</b> binding affinity and <b>(B)</b> specificity analysis.

Figure 5.2	Non-linear binding curves for AptBipD1, AptBipD13, and AptBipD50 with recombinant BipD protein
Figure 5.3	(A) Evaluation of bacterial lysate fractions of <i>B. pseudomallei</i> , including culture supernatant, bacterial supernatant, and bacterial pellet for BipD protein detection through ELONA
Figure 5.4	Specificity analysis of the <b>(A)</b> AptBipD1, <b>(B)</b> AptBipD13 and <b>(C)</b> AptBipD50 against bacterial lysates was analysed through ELONA
Figure 6.1	Workflow for tertiary structural modelling of DNA aptamers142
Figure 6.2	(A) Tertiary structure of predicted BipD protein (AF-Q63K37-F1) visualised using PyMOL (version 2.5)
Figure 6.3	Predicted (A) secondary and (B) tertiary structures of AptBipD1, AptBipD13, and AptBipD50
Figure 6.4	Docked structures of <b>(A)</b> AptBipD1-BipD; <b>(B)</b> AptBipD13-BipD; and <b>(C)</b> AptBipD50-BipD complexes visualised using PyMOL (version 2.5)
Figure 6.5	RMSD of <b>(A)</b> BipD protein and <b>(B)</b> aptamers in the bound state over 100 nanoseconds.
Figure 6.6	RMSF of <b>(A)</b> amino acid residues of the BipD protein and <b>(B)</b> nucleotide residues of aptamers in the bound state over 100 nanoseconds.
Figure 6.7	(A) Rg of BipD protein in the bound state and (B) number of hydrogen bonds between aptamer and BipD protein over 100 nanoseconds159
Figure 6.8	Tertiary structure of AptBipD1-BipD complex following MD simulations
Figure 7.1	Schematic representation of the sequential steps involved in constructing a label-free electrochemical aptasensor for the detection of the BipD protein
Figure 7.2	(A) Cyclic voltammogram for bare SPGEs after activation in 0.5 M sulfuric acid at a scan rate of 100 mV/s

Figure 7.3	Optimisation of thiolated aptamer concentration for immobilisation onto the working surface
Figure 7.4	(A) Square wave voltammogram and (B) bar graph illustrating the progressive decrease in mean peak current during the modification of the electrochemical aptasensor for recombinant BipD protein detection
Figure 7.5	Peak current for the five SPGEs detecting 250 ng/mL of recombinant BipD protein exhibited a range between 74.4 $\mu A$ and 80.0 $\mu A$ , demonstrating the reproducibility of the performance of the electrochemical aptasensor
Figure 7.6	(A) Square wave voltammogram and (B) bar graph showing the specificity analysis of the electrochemical aptasensor using lysates from various bacterial species, including <i>B. pseudomallei</i> , <i>S.</i> Typhi, <i>S. flexneri</i> , <i>E. coli</i> , and <i>K. pneumoniae</i>
Figure 7.7	Linear relationship between changes in mean peak current and log concentration of recombinant BipD protein in (A) 1X PBS, pH 7.4 and (B) spiked serum.

#### LIST OF SYMBOLS

% Percentage

°C Degree Celsius

σ Standard deviation

Δ Change

Å Angstrom

Au Gold

g Gravitational acceleration

Hz Hertz

I Current

K Kelvin

kcal/mol Kilocalories per mole

μ Average

m Slope

μA Microampere

mV Millivolt

mV/s Millivolts per second

*p p*-value

R<sup>2</sup> Coefficient of determination

V Volt

#### LIST OF ABBREVIATIONS

6-MCH 6-mercapto-1-hexanol

μg/mL Microgram per millilitre

μL MicrolitreμM MicromolaraM Attomolarμm Micrometre

AMBER Assisted model building with energy refinement

AMD Active melioidosis detect

ANOVA One-way analysis of variance

API 20 NE Analytical profile index 20 non-enterobacteriaceae

ASSURED Affordable, sensitive, specific, user-friendly, rapid, robust,

equipment-free, and deliverable

B. cepacia Burkholderia cepacia

BimA Burkholderia intracellular motility A

BipB Burkholderia invasion protein B
BipC Burkholderia invasion protein C
BipD Burkholderia invasion protein D

B. mallei Burkholderia mallei

BoaA Burkholderia outer membrane autotransporter protein A
BoaB Burkholderia outer membrane autotransporter protein B
BopE Effector protein of type three secretion system cluster 3

B. pseudomallei Burkholderia pseudomallei

BSA Bovine serum albumin

Bsa Burkholderia secretion apparatus
BsaQ Burkholderia secretion apparatus Q

CASP14 14<sup>th</sup> critical assessment of structure prediction

CDC United States Centers for Disease Control and Prevention

cDNA Complementary DNA

CE Capillary electrophoresis

CFU/mL Colony-forming units per millilitre

CIS Cytokine-inducible Src homology 2-containing protein
CRISPR Clustered regularly interspaced short palindromic repeats

CV Cyclic voltammetry

DALYs Disability-adjusted life-years

DNA Deoxyribonucleic acid

DPV Differential pulse voltammetry

E. coli Escherichia coli

EDC 1-Ethyl-3-(3-dimethylaminopropyl)carbodiimide

EDTA Ethylenediamine tetraacetic acid

EIS Electrochemical impedance spectroscopy

ELISA Enzyme-linked aptamer assay
ELISA Enzyme-linked immunoassay

ELONA Enzyme-linked oligonucleotide assay

fg Femtogram fM Femtomolar

GlcB Glucan Beta-1,3-glucosidase

GroEL Molecular chaperone

GROMACS Groningen machine for chemical simulations

GST Glutathione S-transferase

H<sub>2</sub>S Hydrogen sulphide HCl Hydrochloric acid

Hcp1 Hemolysin co-regulated protein 1

HlyE Hemolysin E

HRP Horseradish peroxidase
HspX Heat shock protein X

HTS High-throughput sequencing ICT Immunochromatography test

IHA Indirect hemagglutination assay

IMAC Immobilised metal affinity chromatography
INFORMM Institute for research in molecular medicine

iNOS Inducible nitric oxide synthase IpaD Needle-tip protein of *Shigella* 

IPTG Isopropyl β-D-1-thiogalactopyranoside

 $K_3[Fe\ (CN)_6]$  Potassium ferricyanide  $K_4[Fe\ (CN)_6]$  Potassium ferrocyanide  $K_d$  Dissociation constant

K. pneumoniae Klebsiella pneumoniae

LAMP-1 Lysosomal-associated membrane protein 1

LAP LC3-associated phagocytosis

LB Luria bertani

LcrV Low-calcium response V

LFA Lateral flow assay

LMICs Low- and middle-income countries

LoD Limit-of-detection

LoQ Limit-of-quantification

M Molar

 $M\Omega$ /cm Megaohms per centimetre

MALDI-TOF MS Matrix-assisted laser desorption ionization-time of flight mass

spectrometry

MD Molecular dynamics

MEGA Molecular evolutionary genetic analysis

mg/mL Milligram per millilitre

mL Millilitre
mM Millimolar
mm Millimetre

MNGC Multinucleated giant cell

MOE Molecular operating environment

MPT64 Secretory protein of Mycobacterium tuberculosis

MRVP methyl red voges-proskauer

M. tuberculosis Mycobacterium tuberculosis

NA Nutrient agar

NAMD Nanoscale molecular dynamics

NB Nutrient broth

NCBI National centre for biotechnology information

ng Nanogram

ng/mL Nanogram per millilitre NHS N-Hydroxysuccinimide

Ni-NTA Nickel-nitrilotriacetic acid

Ni-NTA HRP Nickel-nitrilotriacetic acid horseradish peroxidase

nM Nanomolar nm Nanometre NPT Constant number of particles, pressure, and temperature NVT Constant number of particles, volume, and temperature

OD Optical density

orf2 Open reading frame 2

OTA Ochratoxin A

P. aeruginosaPBSPhosphate-buffered salinePCRPolymerase chain reaction

PEP Post-exposure antimicrobial prophylaxis

pH Potential of hydrogen

pM Picomolar
pmoL Picomole
POC Point-of-care

ProSA Protein structure analysis

psi Pound per square inch PyMOL Python Molecular Viewer

RCSB PDB Research Collaboratory for Structural Bioinformatics Protein

Data Bank

Rg Radius of gyration

RMSD Root mean square deviation

RMSF Root mean square fluctuation

RNA Ribonucleic acid

rpm Revolutions per minute
RSD Relative standard deviation

RT-PCR Real-time polymerase chain reaction

SARS-CoV-2 Severe acute respiratory syndrome coronavirus 2

SAVES Structural analysis and verification server

SDS Sodium dodecyl sulfate

SDS-PAGE Sodium dodecyl sulfate-polyacrylamide gel electrophoresis SELEX Systematic evolution of ligands by exponential enrichment

S. enterica Salmonella enterica
S. flexneri Shigella flexneri

SIM Sulfur, indole and motility

SipD Salmonella invasion protein D

SOC Super optimal broth with catabolite repression

SOCS3 Suppressor of cytokine signaling 3

SPGE Screen-printed gold electrode

S. pneumoniae Streptococcus pneumoniae

SPR Surface plasmon resonance

S. Typhi Salmonella Typhi

SWV Square wave voltammetry

T3SS Type 3 secretion system

T3SS-3 Type 3 secretion system cluster 3

TAE Tris-acetate ethylenediamine tetraacetic acid

TCEP Tris-(2-carboxyethyl) phosphine hydrochloride

TEMED Tetramethylethylenediamine

TMB 3,3',5,5'-Tetramethylbenzidine

TRL Technology Readiness Level

TSI Triple sugar iron

U Unit

UK United Kingdom

USA United States of America

WA Washington

VEGF Vascular endothelial growth factor

Y. pestis Yersinia pestis

#### LIST OF APPENDICES

APPENDIX A PREPARATION OF CHEMICALS AND MEDIA

APPENDIX B LIST OF REAGENTS, CHEMICALS, MEDIA, KITS,

EQUIPMENT AND CONSUMABLES

APPENDIX C SUPPLEMENTARY RESULTS

APPENDIX D ETHICAL APPROVAL

#### PEMBANGUNAN APTAMER DNA TERHADAP ANTIGEN BipD

#### Burkholderia pseudomallei UNTUK APLIKASI DIAGNOSTIK

#### **ABSTRAK**

Melioidosis adalah penyakit yang berjangkit disebabkan oleh Burkholderia pseudomallei (B. pseudomallei). Cabaran utama dalam diagnostik penyakit ini adalah kekangan kaedah piawaian utama yang biasanya memerlukan masa yang lama serta kurang sensitif. Oleh itu, kajian ini bertujuan untuk membangunkan DNA aptamer yang menyasarkan protein invasif Burkholderia D (BipD) untuk aplikasi diagnostik melioidosis. Protein BipD rekombinan telah diekspresikan dan ditulenkan untuk digunakan sebagai sasaran bagi 'systematic evolution of ligands by exponential enrichment' (SELEX). Tiga aptamer telah dipilih berdasarkan frekuensi yang tinggi. Kesemua aptamer terpilih ini dinilai untuk pengikatan affiniti terhadap protein BipD rekombinan, diikuti dengan ujian kekhususan terhadap lisat sel daripada bakteria Gram-negatif lain, termasuk Salmonella Typhi, Shigella flexneri, Escherichia coli dan Klebsiella pneumoniae, melalui ujian oligonukleotida terikat enzim (ELONA). AptBipD1 memaparkan affiniti pengikatan tertinggi, dengan pemalar penceraian (K<sub>d</sub>) sebanyak 0.91 ± 0.08 μM, iaitu lebih rendah berbanding dengan AptBipD13 dan AptBipD50. Ketiga-tiga aptamer menunjukkan kespesifisikan yang kukuh terhadap B. pseudomallei berbanding dengan bakteria lain yang diuji. Analisis pengikatan telah dilakukan melalui kaedah pengiraan seperti 'molecular docking' dan simulasi dinamik molekul. Analisis pengiran menunjukkan bahawa AptBipD1 menunjukkan tenaga pengikatan yang diramalkan tertinggi iaitu -22.8 kcal/mol dan kestabilan yang lebih tinggi apabila mengikat dengan protein BipD, serta tapak pengikatan yang terletak jauh dari hujung 5' dan 3'. Analysis ini menunjukkan bahawa mengimmobilisasi aptamer

ini pada kedua-dua hujung tidak akan menjejaskan ciri pengikatannya. Aptasensor elektrokimia telah dibangunkan dengan mengimmobilisasi aptamer yang paling menjanjikan pada elektrod emas cetak skrin. Aptasensor elektrokimia berasaskan AptBipD1 menunjukkan kespesifikan yang tinggi terhadap *B. pseudomallei* berbanding dengan strain bakteria lain. Sensor ini mempunyai had pengesaan (LoD) sebanyak  $3.4\pm0.03$  ng/mL dan had pengkuantitian (LoQ) sebanyak  $59.2\pm0.03$  ng/mL dalam larutan penampan serta LoD sebanyak  $3.5\pm0.06$  ng/mL dan LoQ sebanyak  $63.2\pm0.06$  ng/mL dalam 'spiked serum'. Ini menunjukkan potensinya untuk pengesanan protein BipD dengan cepat dan tepat, menjadikannya sesuai untuk tujuan diagnostik melioidosis.

# DEVELOPMENT OF DNA APTAMERS AGAINST BipD ANTIGEN OF Burkholderia pseudomallei FOR DIAGNOSTIC APPLICATIONS

#### **ABSTRACT**

Melioidosis is an infectious disease caused by Burkholderia pseudomallei (B. pseudomallei). A major challenge in diagnosing this disease arises from the limitations of the gold standard method, which is often time-consuming and lacks sufficient sensitivity. Therefore, this study aimed to develop DNA aptamers targeting the Burkholderia invasion protein D (BipD) antigen for melioidosis diagnostic applications. The recombinant BipD protein was expressed and purified to serve as the target for DNA aptamer isolation through systematic evolution of ligands by exponential enrichment (SELEX). Three potent aptamers were isolated based on their high frequency. All these selected aptamers were evaluated for their binding affinity to the recombinant BipD protein, followed by specificity testing against lysates from other Gram-negative bacteria, including Salmonella Typhi, Shigella flexneri, Escherichia coli and Klebsiella pneumoniae, through an enzyme-linked oligonucleotide assay (ELONA). AptBipD1 exhibited the highest binding affinity, with a dissociation constant ( $K_d$ ) of  $0.91 \pm 0.08 \mu M$ , which was lower than AptBipD13 and AptBipD50. All three aptamers demonstrated strong specificity for B. pseudomallei compared to other tested bacteria. Binding analyses were performed through computational methods such as molecular docking and molecular dynamics (MD) simulations. Computational analysis revealed that AptBipD1 exhibited the highest predicted binding free energy of -22.8 kcal/mol and greater stability upon binding with BipD protein, as well as the binding site located away from its 5' and 3' ends. This finding suggests that immobilising this aptamer at either end would not affect its binding characteristics. An electrochemical aptasensor was developed by immobilising the most promising aptamer onto screen-printed gold electrodes. AptBipD1-based electrochemical aptasensor demonstrated high specificity for B. pseudomallei over other bacterial strains. This sensor achieved a limit-of-detection (LoD) of  $3.4 \pm 0.03$  ng/mL and limit-of-quantification (LoQ) of  $59.2 \pm 0.03$  ng/mL in buffer, and a LoD of  $3.5 \pm 0.06$  ng/mL and LoQ of  $63.2 \pm 0.06$  ng/mL in spiked serum. The electrochemical aptasensor developed using AptBipD1, which had high binding affinity and specificity, demonstrated low LoD and LoQ in both buffer solution and serum spiked with protein. This indicates its potential for rapid and accurate detection of the BipD protein, making it suitable for diagnostic purposes in melioidosis.

.

#### **CHAPTER 1**

#### INTRODUCTION

#### 1.1 Study background

Melioidosis is a severe and potentially fatal infectious disease caused by the Gram-negative bacterium *Burkholderia pseudomallei* (*B. pseudomallei*). Globally, an estimated 165,000 cases occur each year, with South Asia accounting for 44%. It causes 89,000 deaths annually, with over 99% occurring in low- and middle-income countries (LMICs) (Limmathurotsakul *et al.*, 2016). Melioidosis imposes a substantial health burden, surpassing other tropical diseases such as leptospirosis, dengue, schistosomiasis, lymphatic filariasis, and leishmaniasis (Birnie *et al.*, 2019). It is predominantly endemic in Northern Australia and Southeast Asia, including Malaysia (Gassiep *et al.*, 2020). However, recent studies have identified additional regions of endemicity in Africa, South Asia, and America (Mukhopadhyay *et al.*, 2018; Sanchez-Villamil and Torres, 2018; Steinmetz *et al.*, 2018).

B. pseudomallei is mainly found in moist soil and surface water. It infects humans through three primary routes such as skin inoculation, ingestion of contaminated food or water, and inhalation of contaminated aerosols (Chakravorty and Heath, 2019). Therefore, B. pseudomallei predominantly affects individuals via significant exposure to contaminated soil and water in endemic areas, especially among farmers and those with underlying conditions, notably diabetes (Currie et al., 2021; Zheng et al., 2023). As of now, no vaccine has been developed for melioidosis. The treatment usually starts with an intensive phase using intravenous antibiotics, such as ceftazidime or meropenem, for a duration of two weeks and potentially extending up to eight weeks for severe cases involving arteries or the central nervous system. This is followed by an eradication phase with oral antibiotics such as trimethoprim-

sulfamethoxazole or doxycycline, which lasts a minimum of three months and can extend up to six months, particularly for infections affecting the bones, central nervous system, or arteries (Sullivan *et al.*, 2020).

Melioidosis presents diverse clinical manifestations, ranging from pneumonia to severe septicaemia, often resembling other diseases and complicating accurate and timely diagnosis (Gassiep *et al.*, 2020; Karunanayake, 2022). Consequently, delayed treatment contributes to elevated mortality rates, highlighting the significant public health concern posed by the disease. This underscores the urgent need for advancements in diagnostic methods to improve patient outcomes.

#### 1.2 Problem statement

Currently, diagnosing melioidosis depends on the culture method, which includes enrichment, isolation, and biochemical identification of *B. pseudomallei* from clinical specimens (Lau *et al.*, 2015). Although this method is highly specific, it is time-consuming and often results in false-negative outcomes due to factors such as low bacterial load, prior antibiotic treatment, or inappropriate sample selection (Limmathurotsakul *et al.*, 2010). On the other hand, antibody detection methods serve as an indicator of *B. pseudomallei* exposure, but their utility is hampered by reduced sensitivity and specificity due to elevated background antibodies from prior exposures. As a result, these methods are unable to reliably distinguish between past and current infections (Chaichana *et al.*, 2018). While molecular methods such as conventional polymerase chain reaction (PCR) and real-time PCR (RT-PCR) offer enhanced sensitivity, their application demands specialised equipment, stringent handling procedures, and expert operators (Noparatvarakorn *et al.*, 2023; Radhakrishnan *et al.*, 2021).

In 2014, the Active Melioidosis Detect (AMD) antigen detection kit was developed by InBios International Inc. (Seattle, WA, USA) for the detection of melioidosis. This kit employed a lateral flow assay (LFA) to detect the capsular polysaccharides of *B. pseudomallei*, providing rapid results (Houghton *et al.*, 2014). Extensive evaluation across various clinical samples showed that its sensitivity for blood and serum samples is low, making it unsuitable as a true point-of-care (POC) kit for the detection of melioidosis (Rizzi *et al.*, 2019; Wongsuvan *et al.*, 2018). Moreover, the reliance on antibodies as the molecular recognition elements presents several drawbacks, such as their production requires living hosts, they exhibit batch-to-batch variability, they are temperature-sensitive, and they have a limited shelf life, variability between batches, sensitivity to temperature, and a limited shelf life, making them a less desirable choice for reliable diagnostics (Liu *et al.*, 2022). Hence, there is an urgent demand for a more reliable, rapid, and accurate diagnostic test for melioidosis.

#### 1.3 Rationale of study

This study aims to overcome the limitations of existing diagnostic methods by developing a rapid, accurate, and cost-effective antigen detection test for melioidosis. *Burkholderia* invasion protein D (BipD) antigen of *B. pseudomallei* is a promising diagnostic biomarker. It is a both secreted and needle-tip protein of type 3 secretion system cluster 3 (T3SS-3) that plays essential roles in the pathogenesis of melioidosis by facilitating the invasion of *B. pseudomallei* into host cells, enabling it to escape the phagosome and replicate intracellularly (Gong *et al.*, 2011; Stevens *et al.*, 2003; Stevens *et al.*, 2002). As a virulence factor, the BipD protein is consistently present during infection, making it an ideal candidate for active melioidosis detection. Notably, BipD protein exhibits low sequence similarities with other bacterial proteins,

enhancing the specificity of the diagnostic assay by effectively differentiating melioidosis from other infections (Erskine *et al.*, 2006; Wagner *et al.*, 2023).

Aptamers are single-stranded oligonucleotides that can be either deoxyribonucleic acid (DNA) or ribonucleic acid (RNA). They have unique three-dimensional structures that enable them to bind to specific targets with high affinity. They are commonly called 'chemical antibodies' because they are chemically synthesised and work similarly to antibodies (Domsicova *et al.*, 2024; Mili *et al.*, 2024). Aptamers provide several advantages compared to antibodies, such as cost-effective production, shorter generation time, greater stability, and a longer shelf-life, batch-to-batch uniformity and ease of functionalization (Byun, 2021).

#### 1.4 Scope of study

This study aimed to develop novel DNA aptamers that specifically targeted the BipD protein of *B. pseudomallei* to enhance diagnostic applications for melioidosis. It was structured into five distinct phases. The first phase involved the expression of recombinant BipD protein within an *Escherichia coli* (*E. coli*) system, followed by its purification through affinity chromatography. In the second phase, DNA aptamers targeting the recombinant BipD protein were isolated through agarose-based systematic evolution of ligands by exponential enrichment (SELEX). DNA aptamers from the most enriched SELEX cycle were sequenced and subjected to phylogenetic analysis to identify three aptamers with the highest frequency.

In the third phase, the selected aptamers were characterised using an enzymelinked oligonucleotide assay (ELONA). These aptamers were evaluated for their binding affinity to the recombinant BipD protein, followed by specificity against lysates from other Gram-negative bacteria, including *Salmonella* Typhi (S. Typhi), Shigella flexneri (S. flexneri), E. coli, and Klebsiella pneumoniae (K. pneumoniae). In the fourth phase, binding interaction between the selected aptamers and the BipD protein was predicted through computational methods such as molecular docking and molecular dynamics (MD) simulations. Several parameters were analysed, including binding free energy, stability and binding site of aptamer-BipD complexes. These analyses offered valuable insights into the potential of the aptamers for developing an electrochemical aptasensor.

The final phase focused on assessing the feasibility of developing an electrochemical aptasensor by integrating the most promising aptamer into an electrochemical biosensor platform for real-time detection of BipD protein. In this phase, the screen-printed gold electrode (SPGE) modification was characterised through square wave voltammetry (SWV). The specificity of the electrochemical aptasensor was evaluated for *B. pseudomallei* and other Gram-negative bacteria, as well as the limit-of-detection (LoD) and limit-of-quantification (LoQ) were determined for the recombinant BipD protein in buffer and spiked serum. This study aimed to establish a foundation for a potential diagnostic tool for melioidosis that is rapid, accurate, and cost-effective. The flowchart of the present study is illustrated in Figure 1.1.

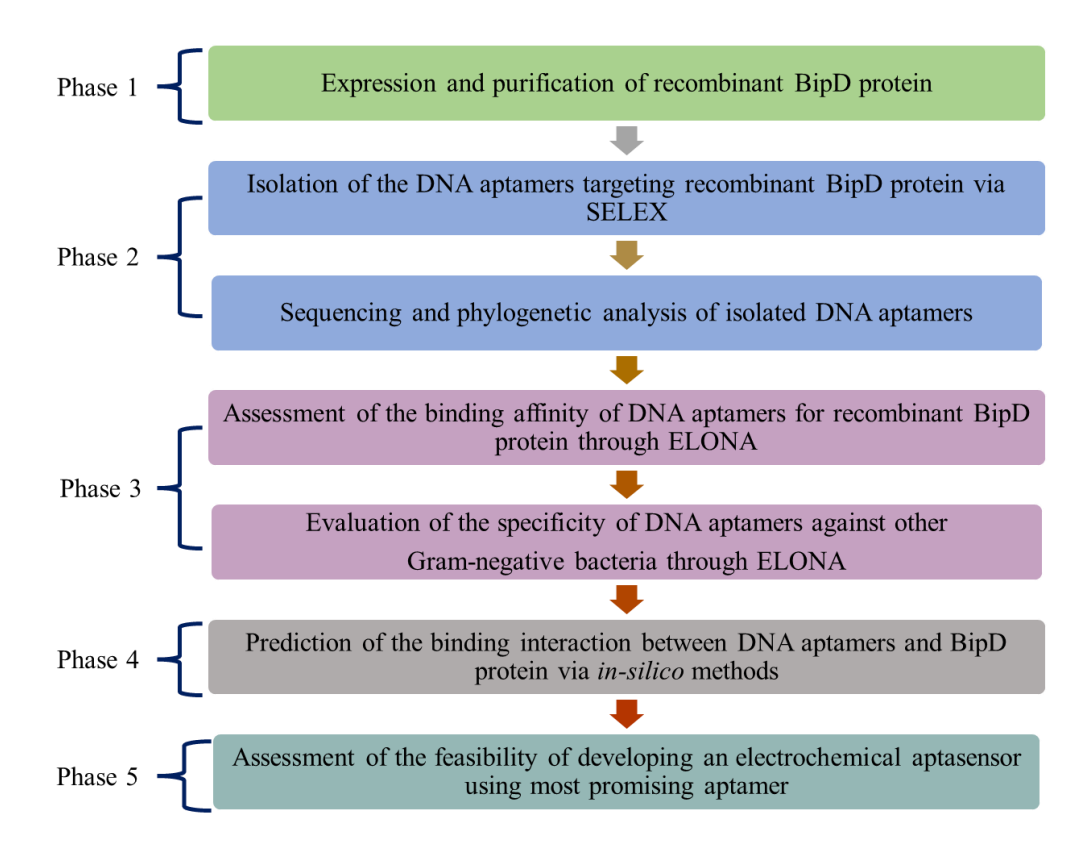


Figure 1.1 Flow chart of the study.

#### 1.5 Study objectives

#### 1.5.1 General objective

The general objective of this study was to isolate DNA aptamers specific to the BipD antigen of *B. pseudomallei* and to develop an electrochemical aptasensor for the diagnosis of melioidosis.

#### 1.5.2 Specific objectives

- 1. To express and purify the recombinant BipD protein.
- 2. To isolate the DNA aptamers targeting the recombinant BipD protein via SELEX.
- 3. To estimate the binding affinity and specificity of the DNA aptamers.
- 4. To predict the binding interaction between the BipD protein and DNA aptamers via *in-silico* methods.
- 5. To develop an electrochemical aptasensor for melioidosis diagnostics.

#### **CHAPTER 2**

#### LITERATURE REVIEW

#### 2.1 Melioidosis: an overview

Melioidosis was first recognised by pathologist Alfred Whitmore and his assistant C. S. Krishnaswami in 1911, among individuals addicted to morphine in Rangoon, Myanmar (Whitmore and Krishnaswami, 1912). The autopsies of these individuals revealed extensive consolidation in the lungs, often accompanied by abscesses in the liver, spleen, or other organs. These findings led to the initial description of the disease as resembling glanders, an equine infection caused by *Burkholderia mallei* (*B. mallei*) (Whitmore, 1913). In 1921, Stanton and Fletcher introduced the term melioidosis, derived from the Greek words 'melis' meaning 'a distemper of asses' and 'eidos' meaning 'resemblance', highlighting its clinical and pathophysiological similarity to glanders (Stanton and Fletcher, 1925).

#### 2.1.1 Global epidemiology of melioidosis

Melioidosis was estimated to affect approximately 165,000 individuals in 2015, among the three billion people living in regions likely to contain *B. pseudomallei*, with an incidence rate of 5.0 per 100,000 individuals at risk annually. Among these cases, 89,000 deaths were estimated, with over 99% occurring in LMICs (Limmathurotsakul *et al.*, 2016). In 2015, the global burden of melioidosis was estimated to be 4.6 million disability-adjusted life-years (DALYs), surpassing other tropical diseases such as intestinal nematode infections (4.56 million DALYs), leptospirosis (2.90 million DALYs), dengue (2.86 million DALYs), and schistosomiasis (2.63 million DALYs) (Birnie *et al.*, 2019). Despite this, the World Health Organisation's new roadmap for neglected tropical diseases from 2021 to 2030

still does not officially recognise melioidosis as a neglected tropical disease (Casulli, 2021).

Regions at the highest risk for melioidosis include Southeast Asia, tropical Australia, South Asia, Western sub-Saharan Africa, and South America (Limmathurotsakul *et al.*, 2016). In Thailand, the annual incidence rate was 3.95 per 100,000 people, with Northeast Thailand reporting the highest rate at 8.73 per 100,000 between 2012 and 2015 (Hantrakun *et al.*, 2019). In the Northern Territory of Australia, annual incidence rates range from 4.8 to 51.2 cases per 100,000 people, with the highest recorded incidence rate among Indigenous Australians reaching 103.6 cases per 100,000 between 2011 and 2012 (Currie *et al.*, 2021). Additionally, in sub-Saharan Africa, around 24,000 melioidosis cases were estimated among six hundred million people living in at-risk regions (Limmathurotsakul *et al.*, 2016).

Recent phylogenetic analysis has revealed that Australia was the original reservoir for the current population of *B. pseudomallei*, which later spread to Southeast Asia, Africa, and America through human migration and cargo transportation (Chewapreecha *et al.*, 2017; Sarovich *et al.*, 2016). Melioidosis cases have also been reported in other regions among returning travellers, with most imported cases in Europe between 2000 and 2018 originating from Southeast Asia, particularly Thailand (53%) (Le Tohic *et al.*, 2019).

Melioidosis remains significantly underreported in approximately 45 countries where it is known to be endemic, as well as in an additional 34 countries that are probably endemic but have never officially reported any cases, as depicted in Figure 2.1 (Limmathurotsakul *et al.*, 2016). Several factors contribute to this neglect. Firstly, the diverse clinical manifestations of melioidosis lead to a lack of awareness among

clinicians and microbiologists, leading to misdiagnosis and inappropriate treatment (Shrestha *et al.*, 2019). Secondly, many LMICs, particularly in remote and rural areas, lack sufficient microbiology services and trained personnel (Savelkoel *et al.*, 2022). Thirdly, there are significant challenges in detecting the bacterium using the gold standard method (Hoffmaster *et al.*, 2015). Finally, the absence of robust national surveillance systems impedes effective monitoring and control of the disease (Nathan *et al.*, 2018).

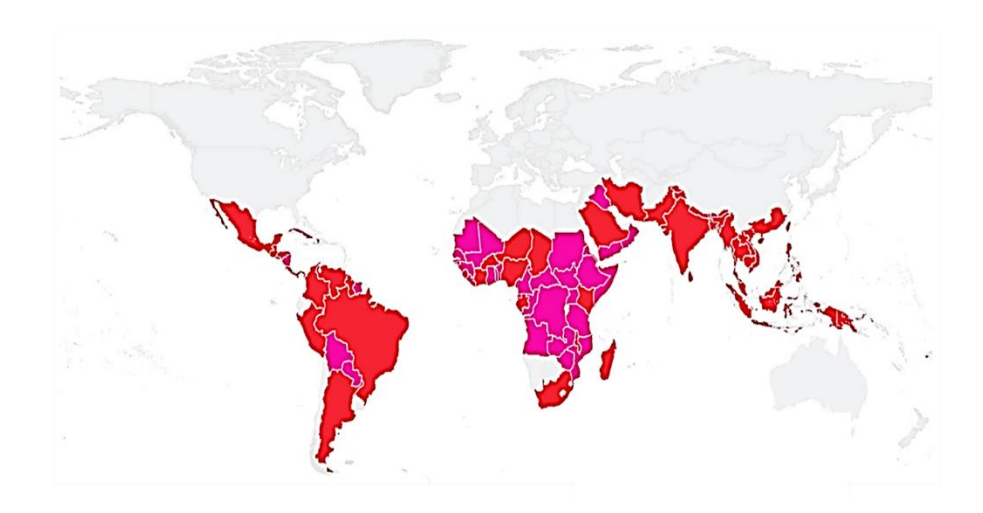


Figure 2.1 Global distribution and reporting of melioidosis. Countries that are endemic for melioidosis but underreported are highlighted in red on the map, while countries predicted to be endemic for melioidosis but remain unreported are shown in pink (Limmathurotsakul *et al.*, 2016).

## 2.1.2 Status of melioidosis in Malaysia

Melioidosis was first reported in Malaysia in 1913, infecting laboratory guinea pigs and rabbits at the Institute for Medical Research (Stanton and Fletcher, 1925). Malaysia is recognised as an endemic country for melioidosis. Currently, it has the second-highest incidence rate of melioidosis in Southeast Asia. Figure 2.2 shows that melioidosis cases in Malaysia are expected to increase, driven by the environmental conditions favourable for *B. pseudomallei* and the rising prevalence of diabetes mellitus, a primary risk factor (Gassiep *et al.*, 2020).

Melioidosis is a notifiable disease in Kedah, Negeri Sembilan and Sabah, but is not recognised nationally under Malaysia's Prevention and Control of Infectious Diseases Act 1988 (Act 342) (Hassan *et al.*, 2010; Hussin *et al.*, 2023; Md Hanif *et al.*, 2024). This lack of nationwide notification complicates efforts to accurately assess the actual impact of melioidosis in the country (Nathan *et al.*, 2018). The annual incidence rate of melioidosis in Malaysia from 2014 to 2020 was 3.41 per 100,000, with significant variations observed between states, as illustrated in Figure 2.3 (Arushothy *et al.*, 2024). It is estimated that over 2,000 patients die from melioidosis annually, a number higher than the deaths caused by dengue or tuberculosis (Nathan *et al.*, 2018).

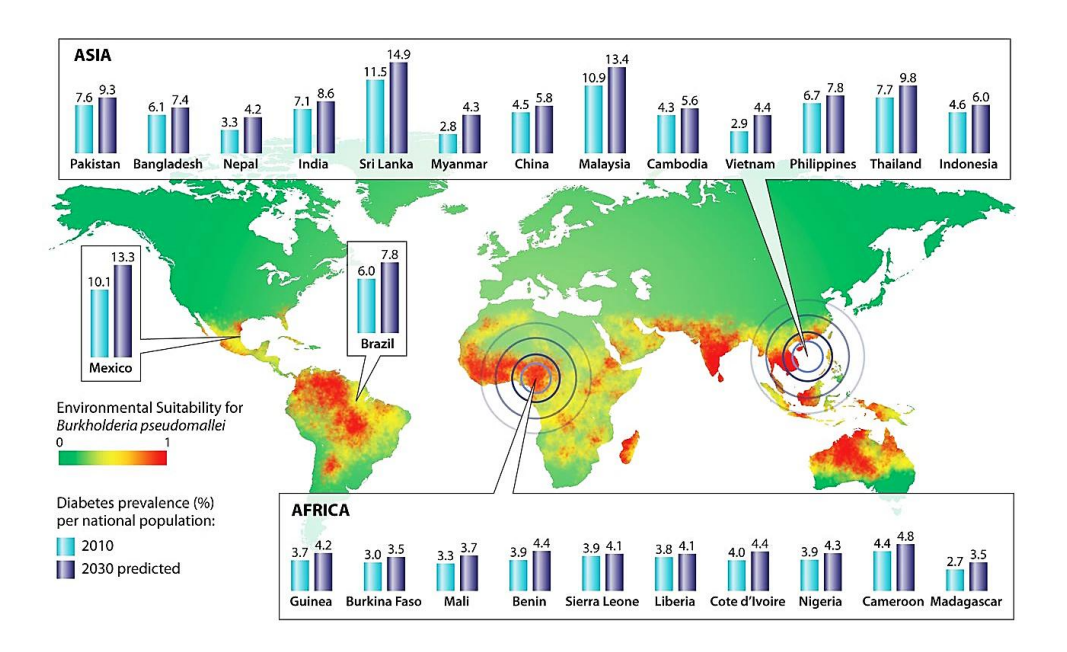


Figure 2.2 Top 25 countries with the highest predicted incidence of melioidosis due to environmental suitability for *B. pseudomallei* and the increase in the prevalence of diabetes mellitus (Gassiep *et al.*, 2020).

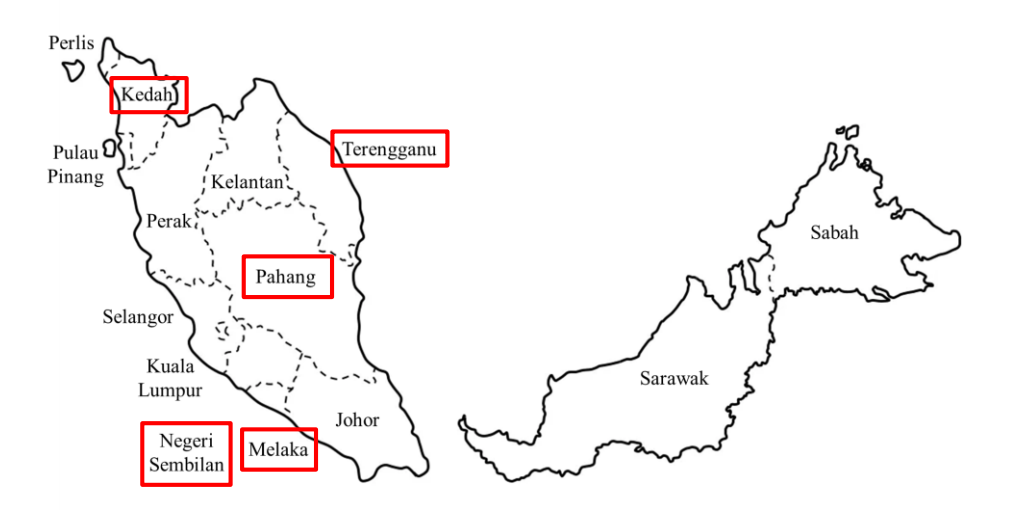


Figure 2.3 States in Malaysia with a high incidence of melioidosis are highlighted in red boxes. Adapted from Arushothy *et al.*, 2024.

In Pahang, the annual incidence rate of melioidosis was 6.1 cases per 100,000 population between 2000 and 2003, with an overall mortality of 54.0% (How *et al.*, 2005). Recent data from 2014 to 2020 showed an increase to 11.33 cases per 100,000 population annually (Arushothy *et al.*, 2024). Kedah reported an annual incidence rate of 16.35 cases per 100,000 population, with a mortality of 33.8% between 2005 and 2008 (Hassan *et al.*, 2010). In Sabah, the annual incidence rate of melioidosis was 4.97 cases per 100,000 population between 2016 and 2018, with a mortality of 28.0% (Hussin *et al.*, 2023). Negeri Sembilan reported an annual incidence rate of melioidosis of 3.1 cases per 100,000 population between 2018 and 2022, with a mortality rate of 0.44 deaths in 100,000 (Md Hanif *et al.*, 2024). In Bintulu, Sarawak, the annual incidence rate of melioidosis was 8.0 cases per 100,000 population between 2008 and 2016 (Fong *et al.*, 2017).

Sarawak exhibited the highest prevalence of melioidosis at 15.1%, while Perlis had the lowest at 0.9% between 2015 and 2019 (Hadi *et al.*, 2021). Kubang Kerian, Kelantan, recorded 158 cases from 2001 to 2015, with a mortality of 32.9% (Zueter *et al.*, 2016). While, Teluk Intan, Perak, 46 cases were recorded from 2013 to 2017 (Tang *et al.*, 2019). Among Malaysian paediatric cases, the reported annual incidence rate of melioidosis ranges from 0.64 to 4.1 cases per 100,000 population (Fong *et al.*, 2015; Mohan *et al.*, 2017).

## 2.2 Etiological agent of melioidosis

The etiological agent of melioidosis is *Burkholderia pseudomallei*, which is an environmental bacterium that has been referred to by various names over the past century, including *Bacillus pseudomallei*, *Bacillus whitmorii*, *Malleomyces pseudomallei*, *Loefflerella pseudomallei*, *Pfeiferella pseudomallei* and *Pseudomonas* 

pseudomallei (Wiersinga et al., 2018). In 1992, based on 16S ribosomal RNA sequences, DNA-DNA homology values, cellular lipid and fatty acid profiles, and distinct phenotypic characteristics, it was reclassified into a newly established genus, Burkholderia, which was named in honour of the American bacteriologist Walter H. Burkholder (Yabuuchi et al., 1992). In 2002, the United States Centres for Disease Control and Prevention (CDC) categorised B. pseudomallei as a Category B agent due to its moderate dissemination, low morbidity and mortality rates and the need for enhanced public health and medical awareness, surveillance, and laboratory diagnostics (Rotz et al., 2002). In 2012, the CDC designated B. pseudomallei as a Tier 1 select agent due to its high potential for deliberate misuse, posing a significant risk of mass casualties, severe economic and infrastructure damage, and a threat to public health and safety (Gassiep et al., 2020).

## 2.2.1 Taxonomy of B. pseudomallei

*B. pseudomallei* is an aerobic, motile and Gram-negative bacillus. It is categorised within the Beta-proteobacteria class, Burkholderiales order and Burkholderiaceae family. The taxonomic classification of the *B. pseudomallei* is detailed in Table 2.1 (Phillips and Garcia, 2024).

Table 2.1 Taxonomy of *B. pseudomallei* (Phillips and Garcia, 2024).

Taxonomic rank	Classification
Domain	Bacteria
Phylum	Pseudomonadota
Class	Betaproteobacteria
Order	Burkholderiales
Family	Burkholderiaceae
Genus	Burkholderia
Species	pseudomallei

## 2.2.2 Classification of *Burkholderia* species

The *Burkholderia* genus encompasses a large group of species, which is further divided into two main clades: Clade I and Clade II (Sawana *et al.*, 2014). Clade I comprises pathogens of humans, animals, and plants such as *B. pseudomallei*, *B. mallei* and *Burkholderia cepacia* (*B. cepacia*). Clade II primarily consist of non-pathogenic plant-associated beneficial and environmental species that have the potential to benefit agriculture. These species are also referred to as *Paraburkholderia* and include *Burkholderia xenovorans*, *Burkholderia terricola* and *Burkholderia fungorum* (Estrada-de los Santos *et al.*, 2013).

## 2.3 Transmission mode of *B. pseudomallei*

*B. pseudomallei* is primarily found in tropical and subtropical regions, thriving in moist, slightly acidic, and nutrient-rich soil as well as surface water (Gassiep *et al.*, 2020). Rice paddies are known to be significant reservoirs for *B. pseudomallei* (Chuah *et al.*, 2017). Notably, *B. pseudomallei* demonstrates an exceptional ability to survive in extreme conditions, including more than 16 years in distilled water, nutrient-depleted soil, and desert (Hantrakun *et al.*, 2016; Pumpuang *et al.*, 2011; Yip *et al.*, 2015). Rivers have been recognised as potential carriers of *B. pseudomallei*. During heavy rainfall, soil containing the bacteria can be washed into the river and possibly transported over long distances to non-endemic areas (Zimmermann *et al.*, 2018).

*B. pseudomallei* causes opportunistic infection in humans via three main routes such as penetration via broken skin, ingestion of contaminated food or water, and inhalation of aerosolised *B. pseudomallei* present in dust or water droplets, as shown in Figure 2.4 (Mohapatra and Mishra, 2022). Skin penetration is the primary mode of transmission, especially in endemic regions where exposure to contaminated soil and

water is common. Farmers, barefoot individuals, and travellers to endemic areas such as Thailand are particularly at risk (Fertitta *et al.*, 2019; Limmathurotsakul *et al.*, 2013). Inhalation of aerosolised *B. pseudomallei* poses a significant risk, as demonstrated by reported cases involving a traveller exposed to dust during a helicopter flight in Singapore and individuals affected during a typhoon in Hong Kong, China (Amadasi *et al.*, 2015; Wu *et al.*, 2023). Ingestion of contaminated drinking water from wells, taps, and boreholes has also been documented as a significant route of *B. pseudomallei* infection (Limmathurotsakul *et al.*, 2014; Tran *et al.*, 2022). However, human-to-human transmission has been exceptionally rare except for cases of mother-to-child transmission that have been documented (Rodríguez *et al.*, 2020; Thatrimontrichai and Maneenil, 2012).

B. pseudomallei also affects various animals such as goats, horses and cattle (Gasqué et al., 2024). However, zoonotic transmission to humans is rare, and veterinarians are considered to be the high-risk group (Virk et al., 2020).

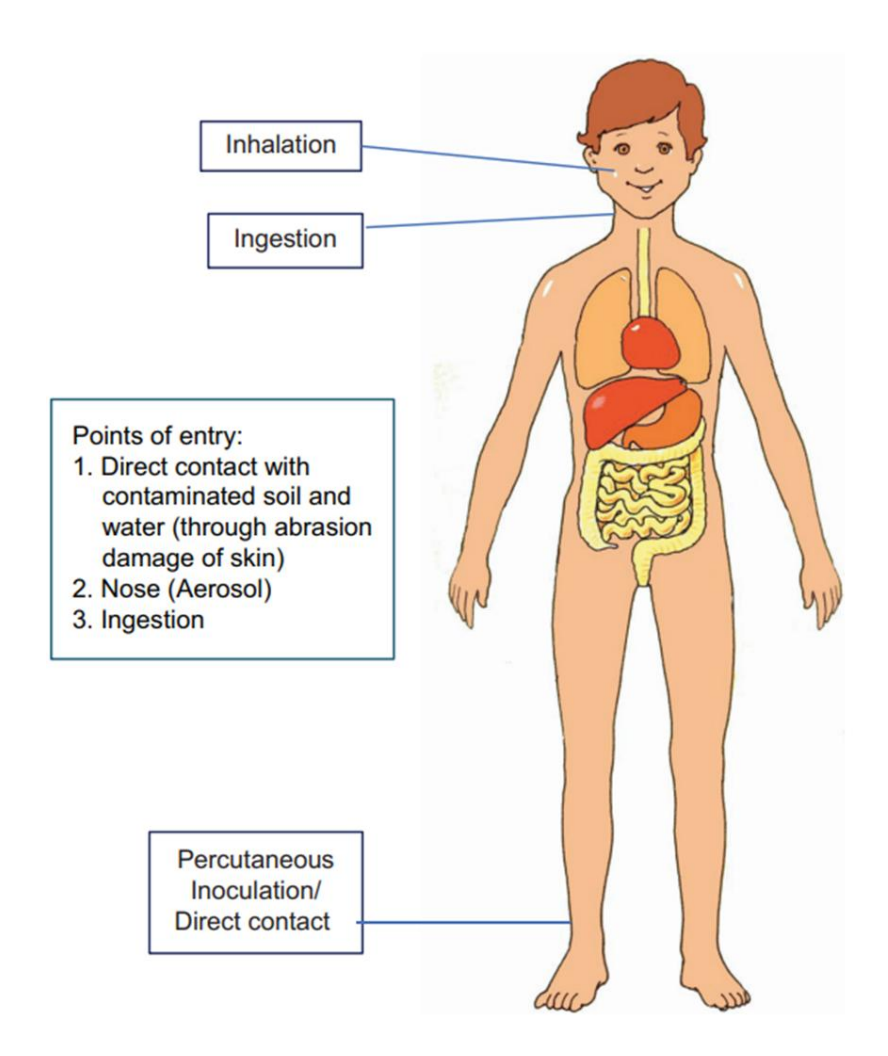


Figure 2.4 Transmission routes of *B. pseudomallei* (Mohapatra and Mishra, 2022). *B. pseudomallei* can enter the human body through three main routes: direct contact with contaminated soil or water via damaged skin (percutaneous inoculation), inhalation of contaminated dust or aerosols, and ingestion of contaminated water or food.

#### 2.4 Risk factors of melioidosis

Diabetes mellitus is the leading risk factor for melioidosis (Birnie *et al.*, 2022; Currie *et al.*, 2021). A meta-analysis revealed that 45.7% of melioidosis patients have diabetes (Chowdhury *et al.*, 2022). Individuals with diabetes are 13 times more likely to contract *B. pseudomallei* infection (Uthaya Kumar *et al.*, 2024). The growing number of people living with diabetes in 2030 will exacerbate the impact of melioidosis outcomes (Gassiep *et al.*, 2020). In addition, hazardous alcohol use is increasingly recognised as a significant risk factor for melioidosis, as it facilitates bacterial dissemination by enhancing barrier permeability and promoting the intracellular invasion of non-phagocytic cells (Jimenez *et al.*, 2018). Furthermore, chronic conditions such as kidney and lung diseases are also risk factors for melioidosis. Among melioidosis patients, the prevalence of chronic kidney disease ranges from 14.6% to 16.9%, while chronic lung diseases range from 12.1% to 28.8% (Chantratita *et al.*, 2023; Sullivan *et al.*, 2020).

Individuals living in endemic areas with frequent exposure to soil and water, such as indigenous Australians (Aboriginal and Torres Strait Islanders), farmers, and military personnel, are at higher risk for *B. pseudomallei* infection (Limmathurotsakul *et al.*, 2016; Nathan *et al.*, 2018; Zheng *et al.*, 2023). Additionally, the incidence rate of melioidosis often rises during extreme weather events (e.g., typhoon) (Wu *et al.*, 2023). Climatic factors such as heavy rainfall, high humidity, and wind speed contribute to the elevated number of melioidosis cases (Bulterys *et al.*, 2018; Currie *et al.*, 2021; Jiee *et al.*, 2023).

# 2.5 Pathogenesis of melioidosis

As a facultative intracellular pathogen, *B. pseudomallei* employs various mechanisms to preserve its survival inside host cells and promote bacterial spread from cell to cell, as presented in Figure 2.5 (Bzdyl *et al.*, 2022).

## 2.5.1 Attachment and invasion of B. pseudomallei

Adhesion of *B. pseudomallei* to host cells is facilitated by polar flagella (Inglis *et al.*, 2003), and type IV pili (Okaro *et al.*, 2022). In addition, type I fimbriae and adhesins such as *Burkholderia* outer membrane autotransporter protein A (BoaA) and *Burkholderia* outer membrane autotransporter protein B (BoaB) promote attachment of *B. pseudomallei* to epithelial cells of the intestine and respiratory tract, respectively (Balder *et al.*, 2010; Sanchez-Villamil *et al.*, 2020). *B. pseudomallei* can invade host cells through two mechanisms. It may invade immune cells, such as macrophages and neutrophils, passively via phagocytosis. Alternatively, it can actively invade non-phagocytic cells, such as epithelial cells (Wiersinga *et al.*, 2018). The T3SS-3 is essential for intracellular invasion of *B. pseudomallei* (Vander Broek and Stevens, 2017), involving several proteins such as BipD and *Burkholderia* secretion apparatus Q (BsaQ) (Kaewpan *et al.*, 2022; Stevens *et al.*, 2003).

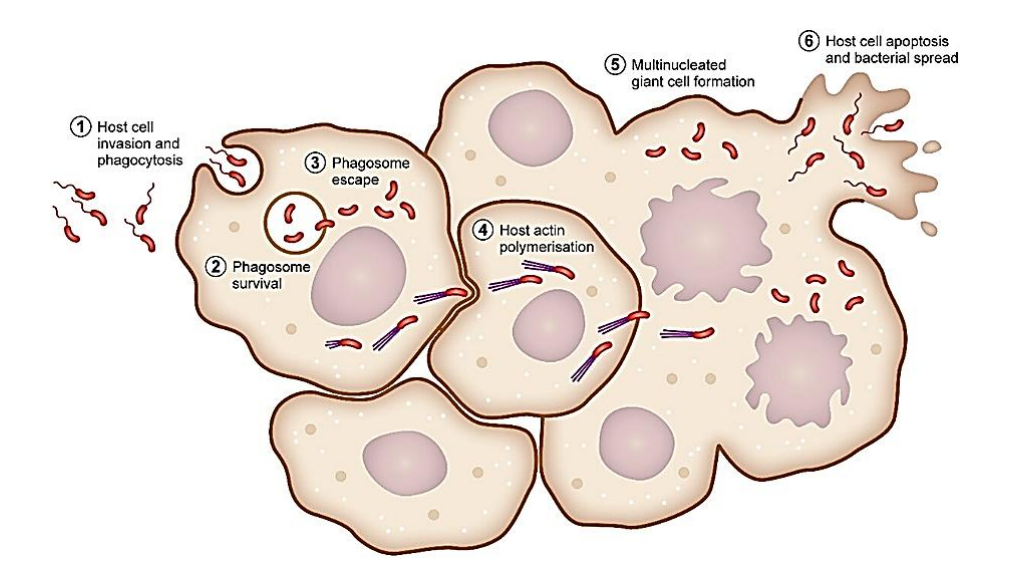


Figure 2.5 Intracellular lifestyle of *B. pseudomallei*. (1) host cell invasion and phagocytosis; (2) phagosome survival, and (3) escape; (4) host actin polymerisation; (5) multinucleated giant cell formation; and (6) host cell apoptosis and bacterial spread (Bzdyl *et al.*, 2022).

# 2.5.2 Phagosomal escape and replication of *B. pseudomallei*

After internalisation by the host cell, *B. pseudomallei* is enclosed in an endocytic vesicle or phagosome, where it can be destroyed when the phagosome fuses with a lysosome. However, *B. pseudomallei* has evolved mechanisms to escape from the phagosome and access the cytoplasm, where it can multiply. It produces a serine protease inhibitor called ecotin, which assists its growth by protecting it from lysosomal degradation (Ireland *et al.*, 2014). *B. pseudomallei* secretes BopE, a T3SS-3 effector protein that suppresses the Rab32-dependent defence pathway, enabling the bacterium to evade phagosomal degradation and persist within host cells (Rao *et al.*, 2024). Additionally, *B. pseudomallei* induces the production of two negative regulators, such as suppressor of cytokine signaling 3 (SOCS3) and cytokine-inducible Src homology 2-containing protein (CIS) in RAW 264.7 macrophage cells. This leads to a reduction in the expression of inducible nitric oxide synthase (iNOS), which is involved in the production of nitric oxide, crucial for the defence and effective clearance of the bacterium (Ekchariyawat *et al.*, 2005).

## 2.5.3 Dissemination and multinucleated giant cell (MNGC) formation

B. pseudomallei utilises actin-mediated motility and membrane protrusions to facilitate intercellular spread. Notably, it possesses the unique protein Burkholderia intracellular motility A (BimA) essential for the formation of actin tails (Jitprasutwit et al., 2023). Following this, host-cell fusion occurs to form MNGC, which is facilitated by hemolysin co-regulated protein 1 (Hcp1) and Burkholderia invasion protein B (BipB) (Kaewpan et al., 2022; Lim et al., 2015). Hcp1 also promotes apoptosis of macrophages, serving as an immune evasion mechanism for B. pseudomallei by preventing the activation of an effective pathogen-clearing response (Stockton et al., 2024). Furthermore, B. pseudomallei can enter the bloodstream,

leading to sepsis. It can also spread to the lymphatic system, facilitating its dissemination to secondary sites.

#### 2.6 Clinical manifestation of melioidosis

B. pseudomallei exhibits a wide array of non-specific clinical manifestations, potentially affecting almost any organ, as depicted in Figure 2.6. Therefore, it is referred to as 'the great mimicker' (Wiersinga et al., 2018). Melioidosis also presents as a subclinical disease with no apparent symptoms in immunocompetent individuals.

#### 2.6.1 Acute infection

The majority of melioidosis cases (85%) present as acute infections following recent exposure to the bacteria. The incubation period ranges from 1 to 21 days (Currie et al., 2021). Individuals diagnosed with acute melioidosis primarily exhibit bacteraemia and pneumonia (Chantratita et al., 2023; Currie et al., 2021). Community-acquired sepsis can occur, but its clinical symptoms are frequently similar to those of other diseases, including malaria, enteric fever, typhus, and leptospirosis (Karunanayake, 2022). The bacteria can also spread through the bloodstream and affect almost any organ, including the lungs, spleen, bone, kidney, skin, liver and brain (Subbalaxmi et al., 2023; Zheng et al., 2023). Interestingly, one of the complications of melioidosis, prostatic abscesses, once considered rare, are now known to be relatively common in Australian patients (Kozlowska et al., 2018). On the other hand, parotitis, another complication of melioidosis, is particularly prevalent among children in Southeast Asia, such as Vietnam and Cambodia, but is rare in Australian children (Chandna et al., 2021; Currie et al., 2021; Pham et al., 2024b).